Title: YB-1, Y-box binding protein-1, is a porter to lead influenza virus ribonucleoprotein complexes to microtubules

Authors: Atsushi Kawaguchi[1, 2], Ken Matsumoto[3, 4], and Kyosuke Nagata[1, *]

Addresses:

[1]Department of Infection Biology, Faculty of Medicine and Graduate School of Comprehensive Human Sciences, University of Tsukuba, 1-1-1 Tennodai, Tsukuba 305-8575, Japan

[2]Kitasato Institute for Life Sciences, Kitasato University, 5-9-1 Shirokane, Minato-ku, Tokyo 108-8641, Japan

[3] Molecular Entomology Laboratory, RIKEN, 2-1 Hirosawa, Wako, Saitama 351-0198, Japan

[4]PRESTO, Japan Science and Technology Agency, 4-1-8 Honcho Kawaguchi, Saitama 322-0012, Japan

[*]Correspondence should be addressed to K. N. (e-mail: knagata@md.tsukuba.ac.jp)

Contact information: Kyosuke Nagata, Department of Infection Biology, Faculty of Medicine and Graduate School of Comprehensive Human Sciences, University of Tsukuba, 1-1-1 Tennodai, Tsukuba 305-8575, Japan Phone: (Japan +81) 29-853-3233, Fax (Japan +81) 29-853-3233, Email: knagata@md.tsukuba.ac.jp

Running title: YB-1 recruits viral RNP complexes to microtubules

Abstract

RNA *de novo* synthesized are under the regulation of multiple post-transcriptional processes by a variety of RNA-binding proteins. The influenza virus genome consists of single-stranded RNAs and exists as viral ribonucleoprotein complexes (vRNP). After the replication of vRNP in the nucleus, vRNP is exported to the cytoplasm and then reaches the budding site beneath cell surface mediated by Rab11a-positive recycling endosomes along microtubules. However, the regulatory mechanisms of post-replicational processes of vRNP are largely unknown. Here, we identified, as a novel vRNP-interacting protein, Y-box binding protein-1 (YB-1), a cellular protein that is involved in regulation of cellular transcription and translation. YB-1 translocated to the nucleus from the cytoplasm and accumulated in PML nuclear bodies in response to influenza virus infection. vRNP assembled into the exporting complexes with YB-1 at PML nuclear bodies. After nuclear-export, using YB-1 knockdown cells and *in vitro* reconstituted systems, YB-1 was shown to be required for the interaction of nuclear-exported vRNP with microtubules around the microtubule organization center (MTOC), where Rab11a-positive recycling endosomes were located. Further, we also found that YB-1 overexpression stimulates the production of progeny virions in an Rab11a-dependent manner. Taken altogether, we propose that YB-1 is a porter that leads vRNP to microtubules from the nucleus and put it on the vesicular trafficking system.

Introduction

In general, RNA transcripts form ribonulceoprotein (RNP) complexes with a number of RNA-binding proteins. The destiny of the RNP complexes in terms of localization, stability, and translational control is regulated by their protein constituents (16, 21, 33).

The genome of influenza type A viruses consists of eight-segmented and single-stranded RNAs of negative polarity (vRNA). vRNA exists as RNP complexes (designated vRNP) with viral RNA-dependent RNA polymerase consisting of three subunits—PB1, PB2, and PA—and nucleoprotein (NP). vRNA is transcribed into mRNA and replicated through cRNA (full-sized complementary copy of vRNA) into a large number of progeny vRNAs in the nucleus (reviewed in 49). The replicated vRNA is assembled into vRNP, and then the progeny vRNP interacts with M1. The vRNP-M1 complex is nuclear-exported through the CRM1-dependent pathway mediated by the interaction of vRNP-M1 complex with NS2 (also called as NEP), which is a viral protein containing an NES (19, 52, 54, 77). After the nuclear-export, it is quite likely that the progeny vRNP accumulates in the microtubule-organizing center (MTOC) and then moves to the budding site beneath the cell surface along microtubules through Rab11a-dependent vesicular trafficking systems (28, 45). Finally, a set of eight segments of vRNA is incorporated into a progeny virion with other viral structural proteins (51, 53, 79).

The Rab11a-positive recycling endosome is important for the delivery of membranes and core polarity proteins to the lateral cell surface (reviewed in 25, 42, 74), leading to the construction of plasma membrane domains and epithelial cell polarity through binding to motor proteins along cytoskeleton (75). The Rab11a-positive

73 recycling endosome is located typically in close proximity to the nucleus and associated
74 with the microtubule organizing center (MTOC). Recent reports demonstrate that a
75 number of viruses, including influenza virus (1, 17, 47), human cytomegalovirus (36),
76 hantavirus (61), respiratory syncytial virus (6, 73), and Sendai virus (9), employ the
77 Rab11a-positive recycling endosomes during the egress. However, the targeting
78 mechanism of cargo molecules including influenza virus vRNP to the Rab11a-positive
79 recycling endosome is still poorly understood.

80 Since influenza virus genome encodes only eleven viral proteins, the virus
81 has to hijack cellular functions/machineries consisting of numerous cellular proteins to
82 achieve every infection processes. Therefore, to understand the regulatory mechanism
83 of the localization and intracellular transport of vRNP, identification and
84 characterization of viral and cellular proteins involved in these processes are required.
85 Here, we identified as a novel vRNP-interacting protein, Y-box binding protein-1
86 (YB-1), a cellular protein that is involved in regulation of cellular transcription and
87 translation (41). In the nucleus, YB-1 functions as a Y-box promoter element-binding
88 transcription factor (34, 37, 41). However, a major portion of YB-1 localizes in the
89 cytoplasm and regulates mRNA translation and degradation as a major component of
90 cellular mRNA ribonucleoprotein (mRNP). A sudden translational arrest in response
91 to a variety of stresses is accompanied by the formation of stress granules (SGs) and an
92 increase in the number of mRNA processing bodies (P-bodies) to reprogram gene
93 expressions post-transcriptionally (3). It is suggested that SGs are aggregates of
94 translationally inactive mRNAs containing stalled translation initiation complexes while
95 P-bodies are mRNP aggregates with proteins involved in mRNA decay and translational
96 repression (2, 21). YB-1 accumulates in these cytoplasmic structures (2) and acts as

either translational activator or inhibitor depending on its amount bound to the target mRNP (55). Therefore, it is proposed that YB-1 determines the fate of cellular mRNPs from their synthesis to destruction.

Here, we found that YB-1 translocates to the nucleus in response to influenza virus infection. The nuclear-imported YB-1 accumulates in nuclear speckles, promyelocytic leukemia nuclear bodies (PML-NBs), together with vRNP, M1, and NS2 in the presence of leptomycin B (LMB), a potent inhibitor of CRM1, suggesting that YB-1 is associated with the vRNP export complexes in the nucleus. At late phases of infection, YB-1 was found in perinuclear granules with the newly synthesized vRNP, and accumulated in Rab11a-positive recycling endosomes along microtubules. Further, we found that YB-1 mediates the interaction of vRNP with microtubules. Collectively, we propose that YB-1 functions as a porter that facilitates the association of the progeny vRNP with microtubules, thereby leading the ride of vRNP onto Rab11a-positivie recycling endosomes.

MATERIALS AND METHODS

Biological materials. vRNP was prepared from purified influenza A/Puerto Rico/8/34 (A/PR/8/34) virus as previously described (66). Rabbit polyclonal antibodies against YB-1, RAP55, RCK, PB1, PB2, PA, M1, and NP, and rat antibody against NS2 were prepared as previously described (30, 31, 40, 50, 71, 72, 77). Rabbit polyclonal antibodies against TIAR, PML (SANTA CRUZ BIOTECHNOLOGY), Rab11a (Invitrogen), and mouse monoclonal antibodies against α-tubulin (Sigma) and PML (SANTA CRUZ BIOTECHNOLOGY) were purchased. Anti-SeV antibody and anti-M1 monoclonal antibody were generously gifted from Dr. A. Kato (National Institute of Infectious Diseases, Japan) and Drs. S. Hongo and K. Sugawara (Yamagata University), respectively. MDCK, 293T, and HeLa cells were grown in Minimal Essential Medium (MEM) containing 10% fetal bovine serum. For the construction of plasmids expressing His-YB-1 and FLAG-α-tubulin, the cDNAs were amplified with a primer set, 5′-GGAATTCCATATGAGCAGCGAGGCCGAGACCCAGC-3′ and 5′-GAACCGCTCGAGCTCAGCCCCGCCCTGCTCAGCCTCGGGAG-3′ for YB-1 and a primer set, 5′-CGCCACCATGGACTACAAGGATGACGACGACAAGCATATGCGTGAGTGCA TCTCC-3′ and 5′-CTATTAATACTCTTCACCCTCAT-3′ for α-tubulin and cDNAs reverse-transcribed from HeLa total RNA using oligo$(dT)_{20}$ primer as a template, respectively. YB-1 cDNA was cloned into pET24b plasmid, and the resultant plasmid was then used as a template to amplify FLAG-YB-1 cDNA with a primer set, 5′-GCCGCCACCATGGACTACAAGGATGACGACGACAAGCATATGAGCAGCGA GGCCGA-3′ and 5′-CCCGGATCCTATTACTCAGCCCCGCCCTG-3′. FLAG-YB-1 and FLAG-α-tubulin cDNAs were cloned into pCAGGS plasmid. The cDNA

fragments of YB-1 deletion mutants were amplified with primer sets, 5′-GCAGATATCATGAGCAGCGAGGCCGA-3′ and 5′-TGCGGATCCCTACCATGGCCCGCCGGCAGGC-3′ for A/P domain (1-50 a.a.), 5′-GCAGATATCATGAGCAGCGAGGCCGA-3′ and 5′-TGCGGATCCTTAACCAGGACCTGTAACATT-3′ for ΔA/B domain (1-129 a.a.), 5′-GCAGATATCGACAAGAAGGTCATCGCAA-3′ and 5′-CCCGGATCCTATTACTCAGCCCCGCCCTG-3′ for ΔA/P domain (51-324 a.a.), and 5′-GCACCATGGGATATCGGTGTTCCAGTTCAAGGC-3′ and 5′-CCCGGATCCTATTACTCAGCCCCGCCCTG-3′ for A/B domain (130-324 a.a.), and then cloned into pGEX-6P plasmid, respectively. To establish HeLa cell lines constitutively expressing either FLAG-YB-1 or FLAG-α-tubulin, HeLa cells transfected with pSV2-Neo and either pCAGGS-FLAG-YB-1 or pCAGGS-FLAG-α-tubulin were selected by growing in the presence of 1 mg/ml G418 for two weeks, and then the G418-resistant colonies were isolated. Recombinant His-YB-1 and GST-fused deletion mutants of YB-1 were purified according to the manufacturer's protocol. In addition, to remove the bacterial RNA possibly bound to YB-1, we treated recombinant YB-1 with RNase A before purification.

LC-MS analysis. Molecular masses of trypsin-digested peptides from co-immunoprecipitated proteins with NP were calculated by liquid chromatography-coupled mass spectrometry (LC-MS) analysis (Thermo) after reduction and alkylation of cysteine residues. Assignment of observed ions was done by Mascot search software.

Cellular localization of viral RNAs and proteins. Indirect immunofluorescence assays and fluorescence *in situ* hybridization (FISH) assays were

161 carried out as previously described (28). Briefly, cells infected with A/PR/8/34 at
162 multiplicity of infection (moi) of 10 were fixed by 1% parafolmaldehyde (PFA) for 5
163 min, and then pre-permeabilized with 0.01% digitonin in PBS for 5 min on ice. After
164 washing with PBS, cells were fixed in 4% PFA for 10 min and permeabilized with 0.5%
165 Triton X-100 in PBS for 5 min on ice. After incubation in PBS containing 1% bovine
166 serum albumin (BSA) for 1 h, coverslips were incubated with each antibody for 1 h, and
167 then with Alexa Fluor 488- or 568-conjugated anti-rabbit, rat, and mouse IgG antibodies
168 (Invitrogen), respectively. After the indirect immunofluorescence assays, FISH assays
169 were performed using RNA probes complementary to the segment 1 vRNA and
170 cRNA/mRNA, respectively. Images were acquired by confocal laser scanning
171 microscope (Zeiss). Each micrograph is a confocal section taken at the same level of
172 focus among samples, so that nuclei were fully observed with a maximum diameter.
173 **Immunoprecipitation.** Infected cells crosslinked with 0.5% formaldehyde
174 for 10 min at room temperature were lysed by sonication in a buffer containing 20 mM
175 Tris-HCl (pH 7.9), 100 mM NaCl, 30 mM KCl, 0.1% NP-40, and 1 mM EDTA. The
176 lysates were subjected to centrifugation at 12,000 xg, and the supernatant fractions were
177 subjected to immunoprecipitation with antibodies where indicated. For detection of
178 viral RNAs immunoprecipitated with YB-1 from infected cells, the immunoprecipitates
179 were subjected to reverse-crosslinking in a buffer containing 50 mM Tris-HCl (pH 7.9),
180 5 mM EDTA, 50 mM DTT, and 1% SDS for 45 min at 70ºC. After
181 reverse-crosslinking, viral RNAs were purified by phenol-chloroform extraction
182 followed by ethanol precipitation, and then reverse-transcribed with primers to
183 determine the level of vRNA (5′-GACGATGCAACGGCTGGTCTG-3′, which
184 corresponds to the segment 5 cRNA between nucleotide sequence positions 424 and

444), cRNA (5′-AGTAGAAACAAGGGTATTTTTCTTTA-3′, which is complementary to the segment 5 cRNA between nucleotide sequence positions 1540 and 1565), and that of viral mRNA (oligo(dT)$_{20}$ for poly(A) tail). The synthesized single-stranded cDNAs were subjected to quantitative real time PCR analysis (Thermal Cycler Dice Real Time System TP800; TaKaRa) with two specific primers, 5′-GACGATGCAACGGCTGGTCTG-3′, which corresponds to the segment 5 cRNA between nucleotide sequence positions 424 and 444, and 5′-AGCATTGTTCCAACTCCTTT-3′, which is complementary to the segment 5 cRNA between nucleotide sequence positions 595 and 614.

Gene silencing mediated by siRNA. Short interfering RNA (siRNA) against *Rab11a* and *YB-1* genes were purchased from Invitrogen, respectively. Cells (5 x 10^5 cells) were transfected with 30 pmol of siRNA using Lipofectamine RNAi MAX (Invitrogen) according to the manufacturer's protocol.

Reconstruction of vRNP-microtubules complex mediated by YB-1. Cellular tubulin and microtubule-associated protein(s) (MAPs) purified from bovine brain as previously described (67) were kindly provided from K. Mizumoto (Kitasato University). The purified tubulin proteins (40 μg) were assembled into microtubules by incubating at 37ºC for 20 min in a buffer containing 50 mM PIPES-NaOH (pH 6.8), 1 mM EGTA, 5 mM $MgCl_2$, 20% Glycerol, 1 mM GTP, and 20 μM Taxol. The reconstituted microtubules were precipitated by centrifugation at 32,000 rpm at 20ºC for 20 min in SW55Ti rotor (Beckman) to remove the monomeric tubulin proteins. The precipitates were resuspended in a buffer containing 50 mM HEPES-NaOH (pH 7.9), 50 mM KCl, 20 μM Taxol, and 0.5% BSA, and then incubated with either vRNP or YB-1-vRNP complexes. The vRNP complexes were immunoprecipitated with anti-NP

209 antibody, and then the co-precipitated microtubules were detected by western blotting
210 assay with anti-α-tubulin antibody.
211

RESULTS

Identification of YB-1 as a novel vRNP-interacting protein. To get further insight in the regulatory mechanism of vRNP function, we tried to determine a novel cellular protein(s) that interacts with vRNP. At 8 h post infection (hpi), infected cell lysates were subjected to immunoprecipitation using anti-NP antibody, and then the precipitated proteins were subjected to LC-MS analysis (Fig. 1A). We found that viral proteins, PB1, PB2, PA, M1, and NS1, were co-precipitated with NP as expected (32, 39, 56, 58, 59), suggesting that not only NP but also vRNP were immunoprecipitated in this experiment. In addition to these viral proteins, we also identified a number of cellular proteins interacting with vRNP as previously reported (Table 1) (29, 43, 44, 46, 76). It is noted that YB-1, a major component of cellular mRNP, was also identified as a novel vRNP-interacting protein. YB-1 regulates the life time and the translational activity of cellular mRNP depending on the amount of YB-1 on a target mRNA (22, 55). Further, it is proposed that YB-1-bound mRNP particles interact with microtubules, but a precise role(s) of YB-1 has not yet been uncovered (11, 12). Thus, we tried to examine whether YB-1 regulates the fate of vRNP.

YB-1 localizes predominantly in the cytoplasm, but translocates to the nucleus to regulate transcription in response to environmental stimuli such as DNA-damaging agents, UV irradiation, hyperthermia, and serum stimulation (34). More importantly, YB-1 is one of the components of SGs and P-bodies, which are cytoplasmic compartments possibly involved in the regulation of translation under stress conditions (78). Viral infection also gives a stressful environment to cells. To elucidate the biological significance of the interaction of vRNP with YB-1, we examined the

236 intracellular localization of YB-1 in influenza virus-infected cells by indirect
237 immunofluorescence assays using anti-YB-1 antibody (Fig. 1B). The vRNA was also
238 counterstained by fluorescence *in situ* hybridization (FISH) method (28). YB-1
239 localized at the cytoplasm in infected cells at 4 hpi as did it in mock-infected cells.
240 Along with the progression of infection, YB-1 was imported to the nucleus and became
241 accumulated in unknown nuclear speckles at 8 hpi. At 12 hpi, a portion of YB-1 was
242 found in unknown cytoplasmic granules with the exported progeny vRNA. Since
243 these cytoplasmic granules of YB-1 were not found in the presence of LMB, a potent
244 inhibitor of CRM1, it is likely that YB-1 is exported with vRNA from the nucleus (Fig.
245 1B). Furthermore, the translocation of YB-1 upon influenza virus infection may not be
246 involved in the innate immunity since the localization of YB-1 was not changed in
247 Sendai virus-infected cells (Fig. 1B). Next, we examined the intracellular localization
248 of RAP55, RCK/p54, and TIAR proteins, which are components of cellular mRNP and
249 accumulate in SGs and P-bodies (2). In contrast to YB-1, we did not find any
250 localization changes of these proteins in response to infection (Fig. 1C). Thus, the
251 translocation of YB-1 found in infected cells may not be involved in a function as a
252 component of SGs and P-bodies.

253 **Interaction of YB-1 with vRNP exporting complexes.** Progeny vRNP is
254 exported to the cytoplasm from the nucleus through the CRM1-dependent pathway by
255 assembling export complexes with viral proteins, M1 and NS2 (19, 52, 54, 77). Since
256 YB-1 may be exported to the cytoplasm together with vRNP, it is assumed that YB-1
257 interacts with vRNP export complexes in the nucleus. To address this, we examined
258 the co-localization of YB-1 with M1 and NS2. We found that M1 but not NS2
259 accumulated in the nuclear speckles with YB-1 at 8 hpi (Fig. 2A). Since a major

portion of the progeny vRNA and NS2 was localized in the cytoplasm (Fig. 1B and 2A), the newly synthesized vRNP may be exported to the cytoplasm immediately after the export complex formation. Thus, we examined the localization of vRNA and NS2 in the LMB-treated cells. By inhibition of the CRM1-dependent export pathway, vRNA was accumulated in the nuclear speckles with YB-1, M1, and NS2 (Fig. 2B). Previously, it was reported that a small portion of M1 and NS2 may localize in PML-NBs (62, 64). It is shown that the overexpression of PML suppresses the influenza virus proliferation (10, 27), suggesting that PML-NBs may contribute to the cellular antiviral response. However, the role of PML-NBs remains controversial since influenza virus replicates normally in cells lacking *PML* gene (20). As expected, in the presence of LMB, we found that vRNA and YB-1 were partially associated with PML-NBs (Fig. 2C). Taken altogether, it is possible that the nuclear-imported YB-1 interacts with the vRNP export complexes in PML-NBs, and then YB-1 is subsequently exported from the nucleus with vRNP.

Influenza virus produces three different RNAs, i.e., vRNA, cRNA, and viral mRNA. Both vRNA and cRNA form ribonucleoprotein complexes with the viral polymerase and NP, whereas vRNA, but not cRNA, is found in the cytoplasm (26) and packaged into the virions. In contrast, the viral mRNA interacts with cellular mRNA-binding proteins, and is exported through the REF/Aly pathway generally used by cellular mRNAs (4, 57). To examine the specific interaction of YB-1 with viral RNAs, we visualized positive-sense RNAs (cRNA and viral mRNA) by FISH assays. The intracellular localization of positive-sense RNAs was not changed by LMB treatment as previously reported (57), and the FISH signals were not co-localized with YB-1 in the absence or presence of LMB (Fig. 3A). Further to show quantitative

284 results, we performed immunoprecipitation assays with cell lysates prepared from cells
285 constitutively expressing FLAG-YB-1 using anti-FLAG antibody as described in
286 MATERIALS AND METHODS. We found that vRNA interacted with YB-1, but
287 neither cRNA nor viral mRNA did in infected cells (Fig. 3B). Thus, it is quite likely
288 that YB-1 is involved in the functional regulation of vRNP, but neither cRNP nor viral
289 mRNP.

290 **Interaction of the YB-1-vRNP complex with Rab11a-positive recycling**
291 **endosomes along microtubules.** At 12 hpi, YB-1 was partially co-localized with the
292 nuclear-exported vRNA in the cytoplasm (Fig. 1B). Recent studies have suggested
293 that the progeny vRNP is transported to the plasma membrane along microtubules via
294 Rab11a-positive recycling endosomes (1, 17, 47). Further, it is reported that YB-1
295 interacts with microtubules (12). Based on these, we examined whether YB-1
296 accumulates in microtubules with vRNP (Fig. 4). We found that the cytoplasmic
297 punctate signals of YB-1 in perinuclear regions were co-localized with α-tubulin (Fig.
298 4A). Then, we examined the interaction of YB-1 with microtubules, Rab11a, and
299 vRNP by immunoprecipitation assays. YB-1 interacted with α-tubulin, but hardly
300 with Rab11a in mock-infected cells (Fig. 4B, lane 3). In contrast, the interaction of
301 YB-1 with Rab11a was significantly increased in infected cells (Fig. 4B, lane 6). To
302 address whether the vRNP-YB-1 complexes accumulate in microtubules with Rab11a,
303 the proteins co-precipitated with YB-1 from infected lysates (Fig. 4B, lane 6) were
304 eluted and then subjected to re-immunoprecipitation with anti-NP antibody (Fig. 4C).
305 Since α-tubulin and Rab11a were immunoprecipitated with anti-NP antibody (Fig. 4C,
306 lane 3), it is quite likely that the progeny vRNP is accumulated on Rab11a-positive
307 recycling endosomes with YB-1 along microtubules.

YB-1 is a positive factor for Rab11a-dependent virus production. It is shown that Rab11a is required for the transport of vRNP to the apical plasma membrane and thereby affects the production of progeny virions (1, 17, 47). Since YB-1 binds to Rab11a together with vRNP (Fig. 4C), it is assumed that YB-1 is involved in production of progeny virions through the Rab11a-positive recycling endosome pathway. To address this, the effect of YB-1 overexpression on the virus titer was examined using siRNA-mediated Rab11a knockdown (KD) cells (Fig. 5). The transfection efficiency was approximately 60%. The amount of exogenously overexpressed FLAG-YB-1 was 3-fold higher than that of endogenous YB-1, and the expression level of Rab11a in KD cells decreased to approximately 30% of that of control cells transfected with the non-targeting siRNA (Fig. 5A). The expression level of viral proteins was found to be virtually unchanged by YB-1 overexpression (Fig. 5B). We found that the amount of infectious virions produced from cells overexpressing YB-1 was significantly increased as compared to cells transfected with empty plasmid, whereas the virus titer was slightly enhanced by YB-1 overexpression in Rab11a KD cells (Fig. 5C). Further, the slopes of the lines in panel C were determined to compare the efficiency of virus production (Fig. 5D). This result shows that the production of infectious viruses was increased by 4.8-fold by the YB-1 overexpression, but the stimulatory activity of YB-1 was reduced by 1.9-fold by Rab11a KD (Fig. 5D). Therefore, it is concluded that YB-1 stimulates the production of infectious viruses in the Rab11a-dependent manner. We also tried to measure the amount of infectious virions produced from YB-1 KD cells. But, YB-1 KD cells tend to die by influenza virus infection after 16-20 hpi (data not shown). Thus, it was difficult to demonstrate the effect of YB-1 on the virus titer using YB-1 siRNA.

YB-1 functions as a porter for vRNP to direct it to microtubules. Figures 4 and 5 suggested that YB-1 functions in the vRNP transport through the Rab11a-positive recycling endosome pathway along microtubules. Next, we tried to demonstrate whether YB-1 functions as a transporter of vRNP to microtubules using siRNA-mediated gene silencing (Fig. 6). At 48 h post transfection of YB-1 siRNA, the expression level of YB-1 in KD cells decreased to 25% of that of control cells (Fig. 6A). There were no differences found in the accumulation level of viral proteins (Fig. 6B), vRNA, and viral mRNA (Fig. 6C) between control and YB-1 KD cells. Previous reports showed that the nuclear-exported vRNP complexes accumulate at MTOC around the perinucleus (45) with Rab11a-positive recycling endosomes (1, 17, 47). We carried out FISH assays to examine whether vRNP complexes localize around the perinucleus in YB-1 KD cells at 8 hpi (Fig. 6D and 6E). A major portion (81.5±7.2%) of vRNA was found as diffusive signals in YB-1 KD cells. Thus, it is quite likely that YB-1 stimulates the accumulation of vRNP at MTOC. As shown in Fig. 2C, the replicated vRNA associated with PML-NBs in the presence of LMB. Since vRNA accumulated in PML-NBs even in YB-1 KD cells with LMB treatment (Fig. 6D), it is strongly suggested that YB-1 is not involved in the association between vRNP and PML-NBs. It is also suggested that YB-1 does not play a role in the vRNP export from the nucleus to the cytoplasm since vRNA was found predominantly in the cytoplasm of YB-1 KD cells (Fig. 6E).

YB-1 interacts with vRNP (Fig. 1A and 4B), but it is unclear whether YB-1 interacts directly with one or more of vRNP components, that is, viral polymerase complexes, NP, and vRNA. To test this, we performed pull-down assays with purified vRNP and His-YB-1 using Ni-NTA resin (Fig. 7A). Not only viral polymerase

356 subunits but also NP were co-precipitated with YB-1 (lane 6), demonstrating that YB-1
357 interacts directly with vRNP. Since YB-1 has a single-stranded RNA binding activity,
358 it is possible that YB-1 binds to vRNA. To address this, vRNP treated with
359 micrococcal nuclease (mnRNP) to deplete vRNA was also subjected to the pull-down
360 assay with His-YB-1. We found that each viral polymerase subunit but not NP from
361 mnRNP was co-precipitated with YB-1 (lane 9), suggesting that YB-1 interacts with
362 viral polymerase complexes. YB-1 consists of three domains: the N-terminal domain,
363 the cold shock domain (CSD), and the C-terminal tail domain. The CSD has the
364 well-characterized RNA-binding motifs RNP-1 and RNP-2, and thereby functions as a
365 nucleic acid-binding domain. The N-terminal domain is rich in alanine and proline
366 (A/P domain), and the C-terminal domain contains alternating clusters of positively and
367 negatively charged amino acid residues (A/B domain). All of the three domains are
368 involved in the interaction with a number of cellular proteins (reviewed in 18). To
369 further characterize the interaction between YB-1 and vRNP, we carried out pull-down
370 assays with GST-fused deletion mutants of YB-1 and vRNP (Fig, 7B). We found that
371 PB1 is co-precipitated with the mutants harboring the A/B domain (lanes 5 and 6; ΔA/P
372 and A/B), suggesting that YB-1 interacts with vRNP through the A/B domain. Next,
373 we tried to demonstrate whether YB-1 recruits vRNP on microtubules *in vitro*.
374 Reconstituted microtubules were incubated with either vRNP or YB-1-vRNP complex,
375 and then subjected to immunoprecipitation using anti-NP antibody (Fig. 7B). We
376 found that microtubules were hardly co-precipitated with vRNP in the absence of YB-1
377 (lane 3). In sharp contrast, in the presence of YB-1, the interaction of vRNP with
378 microtubules was increased by approximately 3-fold (lane 4). Finally, we carried out
379 immunoprecipitation assays with cell lysates prepared from cells constitutively

expressing FLAG-α-tubulin with or without YB-1 KD (Fig. 7C). We found that PB1 was immunoprecipitated with FLAG-α-tubulin from control lysates (lane 3), but slightly from YB-1 KD lysates (lane 6). Therefore, it could be concluded that YB-1 is required for the accumulation of vRNP on microtubules. Taken altogether, we would propose that YB-1 interacts directly with vRNP and functions as a porter that facilitates the binding of vRNP with microtubules, where vRNP is led to Rab11a-positivie recycling endosomes.

388 **DISCUSSION**

389

390 We have identified YB-1, a cellular DNA/RNA-binding protein, as a vRNP-interacting
391 protein (Fig. 1A). YB-1 was found to be relocalized to the nucleus from the cytoplasm
392 and associated with PML-NBs along with the progression of virus infection (Fig. 1B).
393 Previous reports showed that the nuclear-import of YB-1 requires phosphorylation by
394 PKC (35), Jak1 (15), and Akt kinases (69). The other mechanism for nuclear-import
395 of YB-1 is thought to be triggered by a proteolytic cleavage by 20S proteasome to
396 separate the C-terminal fragment (220-324 a.a.) containing a cytoplasmic retention
397 signal (68). When we performed immunofluorescence assays with each antibody
398 recognizing either N-terminus (1-13 a.a.; used in this study) or C-terminus (307-324
399 a.a.; purchased from Sigma), the YB-1 nuclear-import was found only when the
400 antibody recognizing N-terminus was used (data not shown). However, we found that
401 vRNP complexes interact with full-length YB-1 (Fig. 1A), suggesting that the 20S
402 proteasome-mediated processing of YB-1 may not always be required in influenza
403 virus-infected cells. Therefore, it is possible that the recognition specificity of our
404 antibody is due to the unknown conformational change of YB-1 possibly induced by the
405 phosphorylation and/or the interaction with cellular and/or viral proteins.
406 Identification of a signaling pathway and interacting proteins responsible for the
407 nuclear-import of YB-1 upon influenza virus infection is needed.

408 PML-NBs are highly dynamic structures that are disrupted or changed in their
409 morphology in response to environmental stimuli (38). The genomes of several DNA
410 viruses have been shown to be localized and transcribed in the vicinity of PML-NBs (13,
411 23, 24). In most cases, virus-encoded regulatory proteins localize at PML-NBs and

412 disrupt PML-NBs for successful infection, suggesting a negative role for PML-NBs in
413 virus growth (13, 23, 24). In addition to the putative function of PML-NBs during
414 virus infection, it is postulated that PML-NBs are implicated in cellular gene
415 transcription, tumor suppression, proteasomal degradation, cellular senescence,
416 apoptosis, and DNA repair (14, 38). It is proposed that PML-NBs might modulate
417 chromatin architecture and transcription since nascent RNA and several gene loci are
418 found around PML-NBs (5, 13, 65). Given this, it seems likely that viruses hijack this
419 nuclear structure to set up a platform suitable for virus replication. M1 and NS2 were
420 shown to be associated with PML-NBs (62, 64), although the functional significance of
421 the co-localization remains to be determined. We found that the nuclear-imported
422 YB-1 accumulates in PML-NBs, in which vRNA was present with M1 and NS2 when
423 the vRNP export was inhibited (Fig. 2). Therefore, we speculate that the progeny
424 vRNPs could be assembled into the export complexes at PML-NBs and subsequently
425 interact with YB-1. Additional experiments are needed to clarify a precise role(s) of
426 PML-NBs in the vRNP nuclear-export as well as the targeting mechanism of YB-1 to
427 PML-NBs.

428 The accumulation of recycling endosome vesicles around MTOC is disrupted
429 in the presence of microtubule-depolymerization reagents such as nocodazole (8).
430 Thus, it is likely that the intact microtubule functions as a platform for the recycling
431 endosome vesicle. We observed a direct binding of YB-1 with vRNP for the
432 recruitment of vRNP to microtubules (Fig. 7). However, only a small portion of vRNP
433 was co-localized with YB-1 in infected cells, suggesting that YB-1 transiently interacts
434 with vRNP (Fig. 1). Further, we could not find YB-1 in the purified influenza virions
435 (data not shown), suggesting that YB-1 might be dissociated from vRNP prior to

packaging of vRNP into progeny virions. The association between YB-1 and enough amounts of microtubules is proposed to compete with the interaction of YB-1 with cellular mRNP *in vitro* (11). Thus, we speculate that vRNP-YB-1 complexes recruited on microtubules may be disassembled by the microtubule formation, and thereby vRNP could be loaded onto Rab11a-positive recycling endosomes bound to microtubules.

The Rab11a-mediated vesicular transport may be functionally important after arriving at the plasma membrane. For example, the lipid rafts are required for the budding of influenza virus from the apical plasma membrane (63, 70), and cholesterol, an essential component of the lipid rafts, is enriched in the recycling endosome membrane (48). Interestingly, it is shown that influenza virus particles are hardly pinched off from the plasma membranein Rab11a KD cells (7). Thus, it is possible that the Rab11a-positive recycling endosome has an important role in the apical transport of proteins and/or membranes, which are involved in budding process including membrane scission (60). However, it is also possible that the trafficking of the viral genome is required to allow the efficient virus budding. The influenza virus genome consists of eight-segmented vRNA molecules. Since it is believed that the eight individual segments are packaged into a progeny virion (53), a hierarchical incorporation of each vRNA should be required. It is hypothesized that Rab11a-positive transport vesicles might be an assembly center of eight segments of vRNA (17, 47). To further understand the mechanism of influenza virus egress, the dynamics of the recycling endocytic compartment is to be analyzed.

ACKNOWLEDGEMENTS

We thank F Momose (Kitasato University) for helpful discussion, K Mizumoto (Kitasato University), K Irie (University of Tsukuba), T Naiki (University of Tsukuba), A Kato (National Institute of Infectious Diseases, Japan), S Hongo (Yamagata University), and K Sugawara (Yamagata University) for the generous gifts of purified tubulin proteins (K Mizumoto), anti-TIAR antibody (K Irie and T Naiki), anti-SeV antibody (A Kato), and mouse monoclonal anti-M1 antibody (S Hongo and K Sugawara). We also thank M N Asaka (University of Tsukuba), and T Minowa (National Institute for Material Science) for their help for LC-MS analysis. This research was supported in part by a grant-in-aid from the Ministry of Education, Culture, Sports, Science, and Technology of Japan (to KN) and Research Fellowships of the Japanese Society for the Promotion of Science (JSPS) (to AK).

REFERENCES

1. **Amorim, M. J., E. A. Bruce, E. K. Read, A. Foeglein, R. Mahen, A. D. Stuart, and P. Digard.** 2011. A Rab11- and microtubule-dependent mechanism for cytoplasmic transport of influenza A virus viral RNA. J Virol **85:**4143-4156.
2. **Anderson, P., and N. Kedersha.** 2008. Stress granules: the Tao of RNA triage. Trends Biochem Sci **33:**141-150.
3. **Anderson, P., and N. Kedersha.** 2002. Stressful initiations. J Cell Sci **115:**3227-3234.
4. **Bier, K., A. York, and E. Fodor.** 2011. Cellular cap-binding proteins associate with influenza virus mRNAs. J Gen Virol **92:**1627-1634.
5. **Boisvert, F. M., M. J. Hendzel, and D. P. Bazett-Jones.** 2000. Promyelocytic leukemia (PML) nuclear bodies are protein structures that do not accumulate RNA. J Cell Biol **148:**283-292.
6. **Brock, S. C., J. R. Goldenring, and J. E. Crowe, Jr.** 2003. Apical recycling systems regulate directional budding of respiratory syncytial virus from polarized epithelial cells. Proc Natl Acad Sci U S A **100:**15143-15148.
7. **Bruce, E. A., P. Digard, and A. D. Stuart.** 2010. The Rab11 pathway is required for influenza A virus budding and filament formation. J Virol **84:**5848-5859.
8. **Casanova, J. E., X. Wang, R. Kumar, S. G. Bhartur, J. Navarre, J. E. Woodrum, Y. Altschuler, G. S. Ray, and J. R. Goldenring.** 1999. Association of Rab25 and Rab11a with the apical recycling system of polarized Madin-Darby canine kidney cells. Mol Biol Cell **10:**47-61.
9. **Chambers, R., and T. Takimoto.** 2010. Trafficking of Sendai virus nucleocapsids is mediated by intracellular vesicles. PLoS One **5:**e10994.
10. **Chelbi-Alix, M. K., F. Quignon, L. Pelicano, M. H. Koken, and H. de The.** 1998. Resistance to virus infection conferred by the interferon-induced promyelocytic leukemia protein. J Virol **72:**1043-1051.
11. **Chernov, K. G., P. A. Curmi, L. Hamon, A. Mechulam, L. P. Ovchinnikov, and D. Pastre.** 2008. Atomic force microscopy reveals

512 binding of mRNA to microtubules mediated by two major mRNP
513 proteins YB-1 and PABP. FEBS Lett **582:**2875-2881.
514 12. **Chernov, K. G., A. Mechulam, N. V. Popova, D. Pastre, E. S.**
515 **Nadezhdina, O. V. Skabkina, N. A. Shanina, V. D. Vasiliev, A. Tarrade,**
516 **J. Melki, V. Joshi, S. Baconnais, F. Toma, L. P. Ovchinnikov, and P. A.**
517 **Curmi.** 2008. YB-1 promotes microtubule assembly in vitro through
518 interaction with tubulin and microtubules. BMC Biochem **9:**23.
519 13. **Ching, R. W., G. Dellaire, C. H. Eskiw, and D. P. Bazett-Jones.** 2005.
520 PML bodies: a meeting place for genomic loci? J Cell Sci **118:**847-854.
521 14. **Dellaire, G., and D. P. Bazett-Jones.** 2004. PML nuclear bodies:
522 dynamic sensors of DNA damage and cellular stress. Bioessays
523 **26:**963-977.
524 15. **Dooley, S., H. M. Said, A. M. Gressner, J. Floege, A. En-Nia, and P. R.**
525 **Mertens.** 2006. Y-box protein-1 is the crucial mediator of antifibrotic
526 interferon-gamma effects. J Biol Chem **281:**1784-1795.
527 16. **Dreyfuss, G., V. N. Kim, and N. Kataoka.** 2002.
528 Messenger-RNA-binding proteins and the messages they carry. Nat
529 Rev Mol Cell Biol **3:**195-205.
530 17. **Eisfeld, A. J., E. Kawakami, T. Watanabe, G. Neumann, and Y.**
531 **Kawaoka.** 2011. RAB11A is essential for transport of the influenza
532 virus genome to the plasma membrane. J Virol **85:**6117-6126.
533 18. **Eliseeva, I. A., E. R. Kim, S. G. Guryanov, L. P. Ovchinnikov, and D. N.**
534 **Lyabin.** 2011. Y-box-binding protein 1 (YB-1) and its functions.
535 Biochemistry (Mosc) **76:**1402-1433.
536 19. **Elton, D., M. Simpson-Holley, K. Archer, L. Medcalf, R. Hallam, J.**
537 **McCauley, and P. Digard.** 2001. Interaction of the influenza virus
538 nucleoprotein with the cellular CRM1-mediated nuclear export
539 pathway. J Virol **75:**408-419.
540 20. **Engelhardt, O. G., H. Sirma, P. P. Pandolfi, and O. Haller.** 2004. Mx1
541 GTPase accumulates in distinct nuclear domains and inhibits
542 influenza A virus in cells that lack promyelocytic leukaemia protein
543 nuclear bodies. J Gen Virol **85:**2315-2326.
544 21. **Eulalio, A., I. Behm-Ansmant, and E. Izaurralde.** 2007. P bodies: at
545 the crossroads of post-transcriptional pathways. Nat Rev Mol Cell Biol
546 **8:**9-22.
547 22. **Evdokimova, V., P. Ruzanov, H. Imataka, B. Raught, Y. Svitkin, L. P.**

Ovchinnikov, and N. Sonenberg. 2001. The major mRNA-associated protein YB-1 is a potent 5' cap-dependent mRNA stabilizer. EMBO J **20:**5491-5502.

23. **Everett, R. D.** 2006. Interactions between DNA viruses, ND10 and the DNA damage response. Cell Microbiol **8:**365-374.

24. **Everett, R. D., and M. K. Chelbi-Alix.** 2007. PML and PML nuclear bodies: implications in antiviral defence. Biochimie **89:**819-830.

25. **Grant, B. D., and J. G. Donaldson.** 2009. Pathways and mechanisms of endocytic recycling. Nat Rev Mol Cell Biol **10:**597-608.

26. **Herz, C., E. Stavnezer, R. Krug, and T. Gurney.** 1981. Influenza virus, an RNA virus, synthesizes its messenger RNA in the nucleus of infected cells. Cell **26:**391-400.

27. **Iki, S., S. Yokota, T. Okabayashi, N. Yokosawa, K. Nagata, and N. Fujii.** 2005. Serum-dependent expression of promyelocytic leukemia protein suppresses propagation of influenza virus. Virology **343:**106-115.

28. **Jo, S., A. Kawaguchi, N. Takizawa, Y. Morikawa, F. Momose, and K. Nagata.** 2010. Involvement of vesicular trafficking system in membrane targeting of the progeny influenza virus genome. Microbes Infect **12:**1079-1084.

29. **Jorba, N., S. Juarez, E. Torreira, P. Gastaminza, N. Zamarreno, J. P. Albar, and J. Ortin.** 2008. Analysis of the interaction of influenza virus polymerase complex with human cell factors. Proteomics **8:**2077-2088.

30. **Kawaguchi, A., F. Momose, and K. Nagata.** 2011. Replication-coupled and host factor-mediated encapsidation of the influenza virus genome by viral nucleoprotein. J Virol **85:**6197-6204.

31. **Kawaguchi, A., T. Naito, and K. Nagata.** 2005. Involvement of influenza virus PA subunit in assembly of functional RNA polymerase complexes. J Virol **79:**732-744.

32. **Kawakami, K., and A. Ishihama.** 1983. RNA polymerase of influenza virus. III. Isolation of RNA polymerase-RNA complexes from influenza virus PR8. J Biochem **93:**989-996.

33. **Keene, J. D.** 2010. Minireview: global regulation and dynamics of ribonucleic Acid. Endocrinology **151:**1391-1397.

34. **Kohno, K., H. Izumi, T. Uchiumi, M. Ashizuka, and M. Kuwano.** 2003. The pleiotropic functions of the Y-box-binding protein, YB-1. Bioessays

584 **25:**691-698.
585 35. **Koike, K., T. Uchiumi, T. Ohga, S. Toh, M. Wada, K. Kohno, and M.**
586 **Kuwano.** 1997. Nuclear translocation of the Y-box binding protein by
587 ultraviolet irradiation. FEBS Lett **417:**390-394.
588 36. **Krzyzaniak, M. A., M. Mach, and W. J. Britt.** 2009. HCMV-encoded
589 glycoprotein M (UL100) interacts with Rab11 effector protein FIP4.
590 Traffic **10:**1439-1457.
591 37. **Kuwano, M., T. Uchiumi, H. Hayakawa, M. Ono, M. Wada, H. Izumi,**
592 **and K. Kohno.** 2003. The basic and clinical implications of ABC
593 transporters, Y-box-binding protein-1 (YB-1) and angiogenesis-related
594 factors in human malignancies. Cancer Sci **94:**9-14.
595 38. **Lallemand-Breitenbach, V., and H. de The.** 2010. PML nuclear bodies.
596 Cold Spring Harb Perspect Biol **2:**a000661.
597 39. **Martin, K., and A. Helenius.** 1991. Nuclear transport of influenza
598 virus ribonucleoproteins: the viral matrix protein (M1) promotes
599 export and inhibits import. Cell **67:**117-130.
600 40. **Matsumoto, K., H. Nakayama, M. Yoshimura, A. Masuda, N. Dohmae,**
601 **S. Matsumoto, and M. Tsujimoto.** 2012. PRMT1 is required for RAP55
602 to localize to processing bodies. RNA Biol **9**.
603 41. **Matsumoto, K., and A. P. Wolffe.** 1998. Gene regulation by Y-box
604 proteins: coupling control of transcription and translation. Trends Cell
605 Biol **8:**318-323.
606 42. **Maxfield, F. R., and T. E. McGraw.** 2004. Endocytic recycling. Nat Rev
607 Mol Cell Biol **5:**121-132.
608 43. **Mayer, D., K. Molawi, L. Martinez-Sobrido, A. Ghanem, S. Thomas, S.**
609 **Baginsky, J. Grossmann, A. Garcia-Sastre, and M. Schwemmle.** 2007.
610 Identification of cellular interaction partners of the influenza virus
611 ribonucleoprotein complex and polymerase complex using
612 proteomic-based approaches. J Proteome Res **6:**672-682.
613 44. **Momose, F., C. F. Basler, R. E. O'Neill, A. Iwamatsu, P. Palese, and K.**
614 **Nagata.** 2001. Cellular splicing factor RAF-2p48/NPI-5/BAT1/UAP56
615 interacts with the influenza virus nucleoprotein and enhances viral
616 RNA synthesis. J Virol **75:**1899-1908.
617 45. **Momose, F., Y. Kikuchi, K. Komase, and Y. Morikawa.** 2007.
618 Visualization of microtubule-mediated transport of influenza viral
619 progeny ribonucleoprotein. Microbes Infect **9:**1422-1433.

46. **Momose, F., T. Naito, K. Yano, S. Sugimoto, Y. Morikawa, and K. Nagata.** 2002. Identification of Hsp90 as a stimulatory host factor involved in influenza virus RNA synthesis. J Biol Chem **277:**45306-45314.

47. **Momose, F., T. Sekimoto, T. Ohkura, S. Jo, A. Kawaguchi, K. Nagata, and Y. Morikawa.** 2011. Apical Transport of Influenza A Virus Ribonucleoprotein Requires Rab11-positive Recycling Endosome. PLoS One **6:**e21123.

48. **Mukherjee, S., X. Zha, I. Tabas, and F. R. Maxfield.** 1998. Cholesterol distribution in living cells: fluorescence imaging using dehydroergosterol as a fluorescent cholesterol analog. Biophys J **75:**1915-1925.

49. **Nagata, K., A. Kawaguchi, and T. Naito.** 2008. Host factors for replication and transcription of the influenza virus genome. Rev Med Virol **18:**247-260.

50. **Naito, T., F. Momose, A. Kawaguchi, and K. Nagata.** 2007. Involvement of Hsp90 in assembly and nuclear import of influenza virus RNA polymerase subunits. J Virol **81:**1339-1349.

51. **Nayak, D. P., E. K. Hui, and S. Barman.** 2004. Assembly and budding of influenza virus. Virus Res **106:**147-165.

52. **Neumann, G., M. T. Hughes, and Y. Kawaoka.** 2000. Influenza A virus NS2 protein mediates vRNP nuclear export through NES-independent interaction with hCRM1. Embo J **19:**6751-6758.

53. **Noda, T., H. Sagara, A. Yen, A. Takada, H. Kida, R. H. Cheng, and Y. Kawaoka.** 2006. Architecture of ribonucleoprotein complexes in influenza A virus particles. Nature **439:**490-492.

54. **O'Neill, R. E., J. Talon, and P. Palese.** 1998. The influenza virus NEP (NS2 protein) mediates the nuclear export of viral ribonucleoproteins. Embo J **17:**288-296.

55. **Pisarev, A. V., M. A. Skabkin, A. A. Thomas, W. C. Merrick, L. P. Ovchinnikov, and I. N. Shatsky.** 2002. Positive and negative effects of the major mammalian messenger ribonucleoprotein p50 on binding of 40 S ribosomal subunits to the initiation codon of beta-globin mRNA. J Biol Chem **277:**15445-15451.

56. **Portela, A., and P. Digard.** 2002. The influenza virus nucleoprotein: a multifunctional RNA-binding protein pivotal to virus replication. J

Gen Virol **83:**723-734.

57. **Read, E. K., and P. Digard.** 2010. Individual influenza A virus mRNAs show differential dependence on cellular NXF1/TAP for their nuclear export. J Gen Virol **91:**1290-1301.

58. **Rees, P. J., and N. J. Dimmock.** 1981. Electrophoretic separation of influenza virus ribonucleoproteins. J Gen Virol **53:**125-132.

59. **Robb, N. C., G. Chase, K. Bier, F. T. Vreede, P. C. Shaw, N. Naffakh, M. Schwemmle, and E. Fodor.** 2011. The influenza A virus NS1 protein interacts with the nucleoprotein of viral ribonucleoprotein complexes. J Virol **85:**5228-5231.

60. **Rossman, J. S., X. Jing, G. P. Leser, and R. A. Lamb.** 2010. Influenza virus M2 protein mediates ESCRT-independent membrane scission. Cell **142:**902-913.

61. **Rowe, R. K., J. W. Suszko, and A. Pekosz.** 2008. Roles for the recycling endosome, Rab8, and Rab11 in hantavirus release from epithelial cells. Virology **382:**239-249.

62. **Sato, Y., K. Yoshioka, C. Suzuki, S. Awashima, Y. Hosaka, J. Yewdell, and K. Kuroda.** 2003. Localization of influenza virus proteins to nuclear dot 10 structures in influenza virus-infected cells. Virology **310:**29-40.

63. **Scheiffele, P., A. Rietveld, T. Wilk, and K. Simons.** 1999. Influenza viruses select ordered lipid domains during budding from the plasma membrane. J Biol Chem **274:**2038-2044.

64. **Shibata, T., T. Tanaka, K. Shimizu, S. Hayakawa, and K. Kuroda.** 2009. Immunofluorescence imaging of the influenza virus M1 protein is dependent on the fixation method. J Virol Methods **156:**162-165.

65. **Shiels, C., S. A. Islam, R. Vatcheva, P. Sasieni, M. J. Sternberg, P. S. Freemont, and D. Sheer.** 2001. PML bodies associate specifically with the MHC gene cluster in interphase nuclei. J Cell Sci **114:**3705-3716.

66. **Shimizu, K., H. Handa, S. Nakada, and K. Nagata.** 1994. Regulation of influenza virus RNA polymerase activity by cellular and viral factors. Nucleic Acids Res **22:**5047-5053.

67. **Sloboda, R. D., W. L. Dentler, and J. L. Rosenbaum.** 1976. Microtubule-associated proteins and the stimulation of tubulin assembly in vitro. Biochemistry **15:**4497-4505.

68. **Sorokin, A. V., A. A. Selyutina, M. A. Skabkin, S. G. Guryanov, I. V.**

692 **Nazimov, C. Richard, J. Th'ng, J. Yau, P. H. Sorensen, L. P.**
693 **Ovchinnikov, and V. Evdokimova.** 2005. Proteasome-mediated
694 cleavage of the Y-box-binding protein 1 is linked to DNA-damage
695 stress response. EMBO J **24:**3602-3612.
696 69. **Sutherland, B. W., J. Kucab, J. Wu, C. Lee, M. C. Cheang, E. Yorida, D.**
697 **Turbin, S. Dedhar, C. Nelson, M. Pollak, H. Leighton Grimes, K. Miller,**
698 **S. Badve, D. Huntsman, C. Blake-Gilks, M. Chen, C. J. Pallen, and S.**
699 **E. Dunn.** 2005. Akt phosphorylates the Y-box binding protein 1 at
700 Ser102 located in the cold shock domain and affects the
701 anchorage-independent growth of breast cancer cells. Oncogene
702 **24:**4281-4292.
703 70. **Takeda, M., G. P. Leser, C. J. Russell, and R. A. Lamb.** 2003. Influenza
704 virus hemagglutinin concentrates in lipid raft microdomains for
705 efficient viral fusion. Proc Natl Acad Sci U S A **100:**14610-14617.
706 71. **Tanaka, K. J., K. Ogawa, M. Takagi, N. Imamoto, K. Matsumoto, and**
707 **M. Tsujimoto.** 2006. RAP55, a cytoplasmic mRNP component,
708 represses translation in Xenopus oocytes. J Biol Chem
709 **281:**40096-40106.
710 72. **Tay, W. L., G. W. Yip, P. H. Tan, K. Matsumoto, R. Yeo, T. P. Ng, S. D.**
711 **Kumar, M. Tsujimoto, and B. H. Bay.** 2009. Y-Box-binding protein-1 is
712 a promising predictive marker of radioresistance and
713 chemoradioresistance in nasopharyngeal cancer. Mod Pathol
714 **22:**282-290.
715 73. **Utley, T. J., N. A. Ducharme, V. Varthakavi, B. E. Shepherd, P. J.**
716 **Santangelo, M. E. Lindquist, J. R. Goldenring, and J. E. Crowe, Jr.**
717 2008. Respiratory syncytial virus uses a Vps4-independent budding
718 mechanism controlled by Rab11-FIP2. Proc Natl Acad Sci U S A
719 **105:**10209-10214.
720 74. **van Ijzendoorn, S. C.** 2006. Recycling endosomes. J Cell Sci
721 **119:**1679-1681.
722 75. **Wakabayashi, Y., P. Dutt, J. Lippincott-Schwartz, and I. M. Arias.**
723 2005. Rab11a and myosin Vb are required for bile canalicular
724 formation in WIF-B9 cells. Proc Natl Acad Sci U S A **102:**15087-15092.
725 76. **Watanabe, K., T. Fuse, I. Asano, F. Tsukahara, Y. Maru, K. Nagata, K.**
726 **Kitazato, and N. Kobayashi.** 2006. Identification of Hsc70 as an
727 influenza virus matrix protein (M1) binding factor involved in the

virus life cycle. FEBS Lett **580:**5785-5790.

77. **Watanabe, K., N. Takizawa, M. Katoh, K. Hoshida, N. Kobayashi, and K. Nagata.** 2001. Inhibition of nuclear export of ribonucleoprotein complexes of influenza virus by leptomycin B. Virus Res **77:**31-42.

78. **Yang, W. H., and D. B. Bloch.** 2007. Probing the mRNA processing body using protein macroarrays and "autoantigenomics". RNA **13:**704-712.

79. **Zhang, J., A. Pekosz, and R. A. Lamb.** 2000. Influenza virus assembly and lipid raft microdomains: a role for the cytoplasmic tails of the spike glycoproteins. J Virol **74:**4634-4644.

741 **FIGURE LEGENDS**

742

743 **FIG 1** Identification of YB-1 as a novel vRNP-interacting proteins. (A)
744 Identification of cellular and viral proteins interacting with vRNP complexes. HeLa
745 cells infected with influenza virus at moi of 10 were subjected to immunoprecipitation
746 assays with control IgG- (lane 2) or anti-NP (lane 3) antibody-conjugated protein
747 A-Sepharose. The co-precipitated proteins were eluted in 100 mM glycine (pH 2.8),
748 separated through 10% SDS-PAGE, and visualized by silver staining. Molecular
749 weight markers are also shown in lane 1. (B) Intracellular localization of YB-1 in
750 infected cells. Infected MDCK cells were subjected to indirect immunofluorescence
751 assays with anti-YB-1 antibody followed by FISH assays using a probe that hybridizes
752 with segment 1 vRNA at 0, 4, 8, and 12 hpi. For LMB treatment, infected cells were
753 incubated in culture medium containing 20 nM LMB at 7 hpi, and then the intracellular
754 localization of vRNA and YB-1 was visualized by FISH and indirect
755 immunofluorescence assays at 12 hpi. The result of SeV-infected cells at 12 hpi is also
756 shown. Scale bar, 10 μm. (C) Intracellular localization of cellular proteins related to
757 P-bodies and SGs. Mock-infected (left panels) or infected MDCK cells at 8 hpi (right
758 panels) were subjected to indirect immunofluorescence assays with anti-RAP55 (upper
759 panels, red), anti-RCK (middle panels, red), and anti-TIAR (lower panels, red)
760 antibodies, respectively. Nuclear DNA was stained with TO-PRO-3 iodide (blue).
761 Scale bar, 10 μm.

762

763 **FIG 2** Co-localization of YB-1 and vRNP export complexes in nuclear speckles. (A)
764 Intracellular localization of YB-1, M1, and NS2. At 8 hpi, infected MDCK cells were

765 subjected to indirect immunofluorescence assays with rabbit anti-YB-1 (red) and either
766 mouse anti-M1 (upper panel, green) or rat anti-NS2 (lower panel, green) antibody.
767 Scale bar, 10 μm. (B) Intracellular localization of vRNA, YB-1, M1, and NS2 in the
768 presence of LMB. At 7 hpi, infected MDCK cells were incubated for 1 h in the
769 presence of 20 nM of LMB. Segment 1 vRNA (left panels, green), YB-1 (upper panel,
770 red), M1 (middle panel, red), and NS2 (lower panel, red) were visualized by FISH and
771 indirect immunofluorescence assays, respectively. Scale bar, 10 μm. (C)
772 Accumulation of vRNA and YB-1 in PML-NBs in the presence of LMB. After
773 treatment of LMB as described in panel B, mock-infected (upper panel) and infected
774 (middle and lower panels) MDCK cells were subjected to FISH assays using the probe
775 that hybridizes with segment 1 vRNA (upper and middle panels, green) and the indirect
776 immunofluorescence assays with rabbit (upper and middle panels, red) and mouse
777 (lower panel, red) anti-PML and rabbit anti-YB-1 antibodies (lower panel, green),
778 respectively. Scale bar, 10 μm.
779
780 **FIG 3** Specific interaction of YB-1 with vRNA but neither cRNA nor viral mRNA.
781 (A) Intracellular localization of YB-1 and viral mRNA/cRNA. At 8 hpi, infected
782 MDCK cells were subjected to FISH assays using a probe that hybridizes with segment
783 1 cRNA and mRNA (green) and indirect immunofluorescence assays with anti-YB-1
784 antibody (red) with or without 20 nM LMB treatment for 1 h. Nuclear DNA was
785 stained with TO-PRO-3 iodide (blue). Scale bar, 10 μm. (B)
786 Co-immunoprecipitation of YB-1 and viral RNA molecules. HeLa cells constitutively
787 expressing FLAG-YB-1 were infected with influenza virus at moi of 10. After 8 hpi,
788 cell lysates were prepared and subjected to immunoprecipitation assays in the presence

789 of either control IgG or anti-FLAG antibody as described in Methods. The
790 immunoprecipitated viral RNAs were eluted with 100 μg/ml FLAG peptide, and then
791 quantitatively analyzed by reverse transcription followed by real-time PCR with primers
792 specific for segment 5 vRNA, cRNA, and *NP* mRNA, respectively. To quantitatively
793 evaluate, 5%-equivalents of mock-infected and infected samples were also observed.
794
795 **FIG 4** Accumulation of YB-1-vRNP complexes on microtubules with
796 Rab11a-positive recycling endosomes in response to infection. (A) Co-localization of
797 YB-1 and microtubules in cytoplasmic punctate signals. At 12 hpi, mock-infected
798 (upper panels) and infected MDCK cells (lower panels) were subjected to indirect
799 immunofluorescence assays with anti-YB-1 (red) and α-tubulin (green) antibodies.
800 Scale bar, 10 μm. (B and C) Interaction of YB-1 with Rab11a-positive recycling
801 endosomes on microtubules. HeLa cells constitutively expressing FLAG-YB-1 were
802 infected with influenza virus at moi of 10. Cell lysates were prepared and subjected to
803 immunoprecipitation assays in the presence of either control IgG (panel B, lanes 2 and
804 5) or anti-FLAG antibody (panel B, lanes 3 and 6) at 12 hpi. Co-precipitated proteins
805 were eluted with 100 μg/ml FLAG peptide and detected by western blotting assays with
806 anti-PB1, anti-Rab11a, anti-α-tubulin, and anti-FLAG antibodies. The
807 10%-equivalents of mock-infected (panel B, lane 1) and infected lysates (panel B, lane
808 4) were also subjected to western blotting assays. Further, the eluate purified from
809 infected lysate (panel B, lane 6) was re-immunoprecipitated with either control IgG
810 (panel C, lane 2) or anti-NP antibody (panel C, lane 3), and then the eluate was
811 subjected to western blotting assays with anti-α-tubulin and anti-Rab11a antibodies.
812 Panel C, lane 1 represents the 30%-equivalent of proteins immunopurified with

anti-FLAG antibody from infected cell lysate.

FIG 5 The effect of YB-1 overexpression on the production of infectious virions. (A) Expression level of YB-1 and Rab11a proteins. 293T cells were transfected with either pCAGGS empty plasmid (lanes 1 and 3) or pCAGGS-FLAG-YB-1 (lanes 2 and 4) after 24 h post treatment of either non-targeting (control; lanes 1 and 2) or Rab11a siRNA (siRab11a; lanes 3 and 4). After 24 h post transfection of expression vectors, the cell lysates were prepared and analyzed by SDS-PAGE followed by western blotting assays with anti-YB-1, anti-Rab11a, and anti-β-actin antibodies. (B) The accumulation level of viral proteins in cells overexpressing FLAG-YB-1. 293T cells were transfected with either pCAGGS or pCAGGS-FLAG-YB-1. At 24 h post transfection, cells were infected with influenza virus at moi of 10. At 0, 2, 5, and 8 hpi, cell lysates were prepared and analyzed by western blotting assays with anti-PB1, anti-NP, anti-M1, anti-NS2, and anti-α-tubulin antibodies. (C) Production of infectious virions. Control (open diamonds and filled squares) and Rab11a KD 293T (open triangles and open squares) cells transfected with either pCAGGS (open diamonds and open triangles) or pCAGGS-FLAG-YB-1 (filled and open squares) as described in panel A were infected with influenza virus at moi of 0.5. The culture supernatants collected at 3, 6, 12, 16, 20, and 24 hpi were subjected to plaque assays to examine the production of infectious virions in a single-round infection. The average titers and standard deviations determined from three independent experiments are shown. (D) Stimulatory activity of YB-1 on the virus titer in Rab11a KD cells. The slopes of the lines in panel C were determined by the least-square method, and the ratio of the virus titer from cells overexpressing FLAG-YB-1 to that from cells transfected

837 with pCAGGS is shown.

838

839 **FIG 6** Acumulation of vRNP on microtubules in YB-1 knockdown cells. (A) The
840 expression level of YB-1 in YB-1 KD cells. HeLa cells transfected with non-targeting
841 (Control; lanes 1-4) or YB-1 siRNA (siYB-1; lanes 5-8) were lysed, and then the lysates
842 (2.5×10^3, 5×10^3, 1×10^4, and 2×10^4 cells) were subjected to SDS-PAGE followed by
843 western blotting assays with anti-YB-1 antibody at 48 h post transfection. (B and C)
844 The accumulation level of viral proteins and RNAs in YB-1 KD cells. At 48 post
845 transfection of siRNA, control and YB-1 KD cells were infected with influenza virus at
846 moi of 10. After 0, 2, 5, and 8 hpi, cell lysates were prepared and analyzed by western
847 blotting assays with anti-PB1, anti-NP, anti-M1, anti-NS2, and anti-α-tubulin antibodies
848 (panel B). Total RNAs purified from the cells at 0, 2, 5, and 8 hpi were subjected to
849 reverse transcription followed by quantitative real-time PCR with primers specific for
850 segment 5 vRNA and *NP* mRNA as described in Materials and Methods. (D and E)
851 Intracellular localization of vRNA in YB-1 KD cells. At 8 hpi with or without LMB
852 treatment for 1 h, infected control and YB-1 KD cells were subjected to FISH assays
853 using a probe that hybridizes with segment 1 vRNA (panel D; scale bar=10 μm). Cells
854 were counted, and the localization pattern of vRNA in the absence of LMB was
855 determined (panel E). The number of cells showing each localization pattern was
856 expressed as the percentage of the total cell number (*n*=80) in panel E. The average
857 percentages determined from three independent experiments are shown

858

859 **FIG 7** YB-1 functions as a porter bringing the progeny vRNP to microtubules. (A)
860 Direct interaction of YB-1 with viral polymerase complex. The vRNP (lanes 4-6) or

861 micrococcal nuclease-treated vRNP (mnRNP; lanes 7-9) were incubated in the absence
862 (lanes 2, 5, and 8) or presence of purified recombinant His-YB-1 protein (lanes 3, 6, and
863 9) at 30ºC for 1 h. Complexes were purified using Ni-NTA resin, and then proteins
864 were separated through SDS-PAGE and detected by CBB staining and western blotting
865 assays with anti-PB1, anti-PB2, and anti-PA antibodies. Lanes 1, 4, and 7 represent
866 20% of input amounts. (B) Interaction of vRNP with deletion mutants of YB-1.
867 Each GST-fused deletion mutant of YB-1 was incubated with vRNP at 30ºC for 1 h.
868 Complexes were purified using glutathione-Sepharose resins, and then proteins were
869 separated through SDS-PAGE and detected by western blotting assays using anti-PB1
870 antibody. Lane 1 represents 20% of input amounts. Schematic diagram of the
871 deletion mutants of YB-1 is indicated at the bottom. (C) The interaction between
872 vRNP and microtubules mediated by YB-1. Reconstituted microtubules were
873 incubated with either vRNP (lanes 2 and 4) or YB-1-vRNP complex (lanes 3 and 5), and
874 then complexes were immunoprecipitated with either a non-specific IgG (control; lanes
875 2 and 3) or anti-NP antibody (lanes 4 and 5). The immunoprecipitated proteins were
876 separated through SDS-PAGE and subjected to western blotting assays with
877 anti-α-tubulin and anti-NP antibodies. Lane 1 represents 10% of input amount. (D)
878 Interaction of vRNP with microtubules in YB-1 KD cells. HeLa cells constitutively
879 expressing FLAG-α-tubulin were infected with influenza virus at moi of 10. At 8 hpi,
880 the cell lysates were prepared and subjected to immunoprecipitation assays with either
881 control IgG or anti-FLAG antibody. The immunoprecipitated proteins eluted with 100
882 μg/ml FLAG peptide were separated through SDS-PAGE, and then visualized by
883 western blotting assays using anti-PB1 and anti-α-tubulin antibodies. The
884 5%-equivalents of control (lane 1) and YB-1 KD lysates (lane 4) are also shown.

885 **Table 1.** LC-MS analysis of vRNP-interacting proteins.

Protein name	No. of observed peptides	Mascot score	Sequence coverage (%)
Heterogenous nuclear ribonucleorpotein A1	6	85	9
Heterogeneous nuclear ribonucleoproteins C1/C2	11	64	21
Heterogeneous nuclear ribonucleoprotein D0	4	77	12
Heterogeneous nuclear ribonucleoprotein H	9	159	17
Heterogeneous nuclear ribonucleoprotein H2	8	111	17
Heterogeneous nuclear ribonucleoprotein L	7	98	17
ATP-dependent RNA helicase DDX3Y	15	80	17
ATP-dependent RNA helicase DDX5	7	81	10
ATP-dependent RNA helicase DDX17	10	87	12
Nucleolin	8	85	13
78 kDa glucose-regulated protein	11	157	15
Importin subunit alpha-7	3	65	8
Y-box binding protein-1	3	91	10
Tubulin alpha-1C chain	5	70	12
Spliceosome RNA helicase UAP56	5	62	10
Heat shock protein 90 alpha	9	111	15
Heat shock protein 90 beta	9	73	14
Heat shock cognate 71 kDa protein	11	134	15
Heat shock 70 kDa protein 1	12	120	14

886

887

Kawaguchi et al., Figure 1

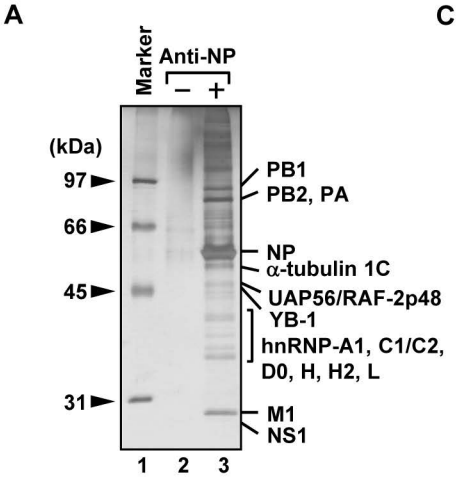

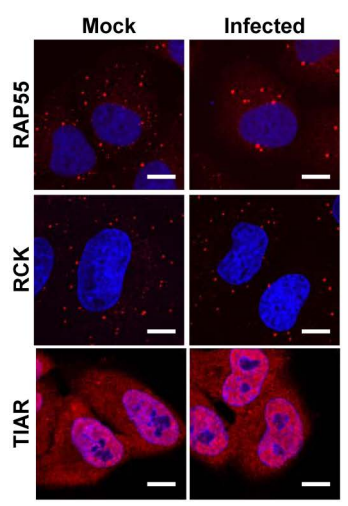

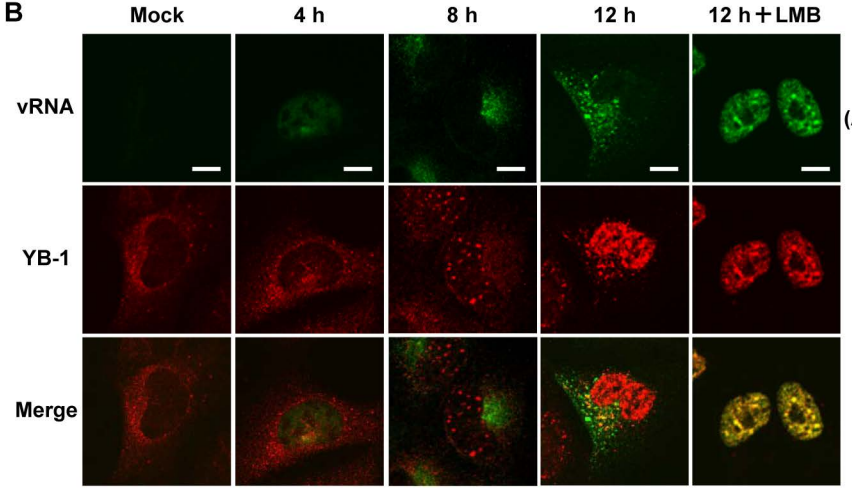

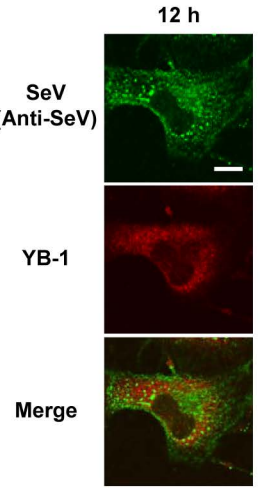

Kawaguchi et al., Figure 2

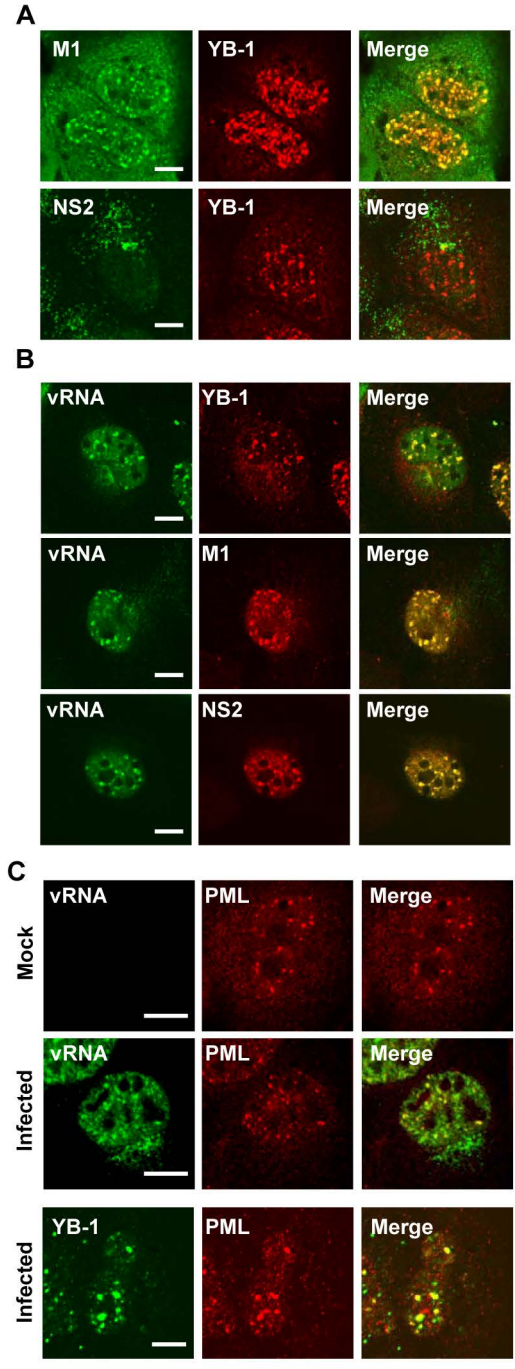

Kawaguchi et al., Figure 3

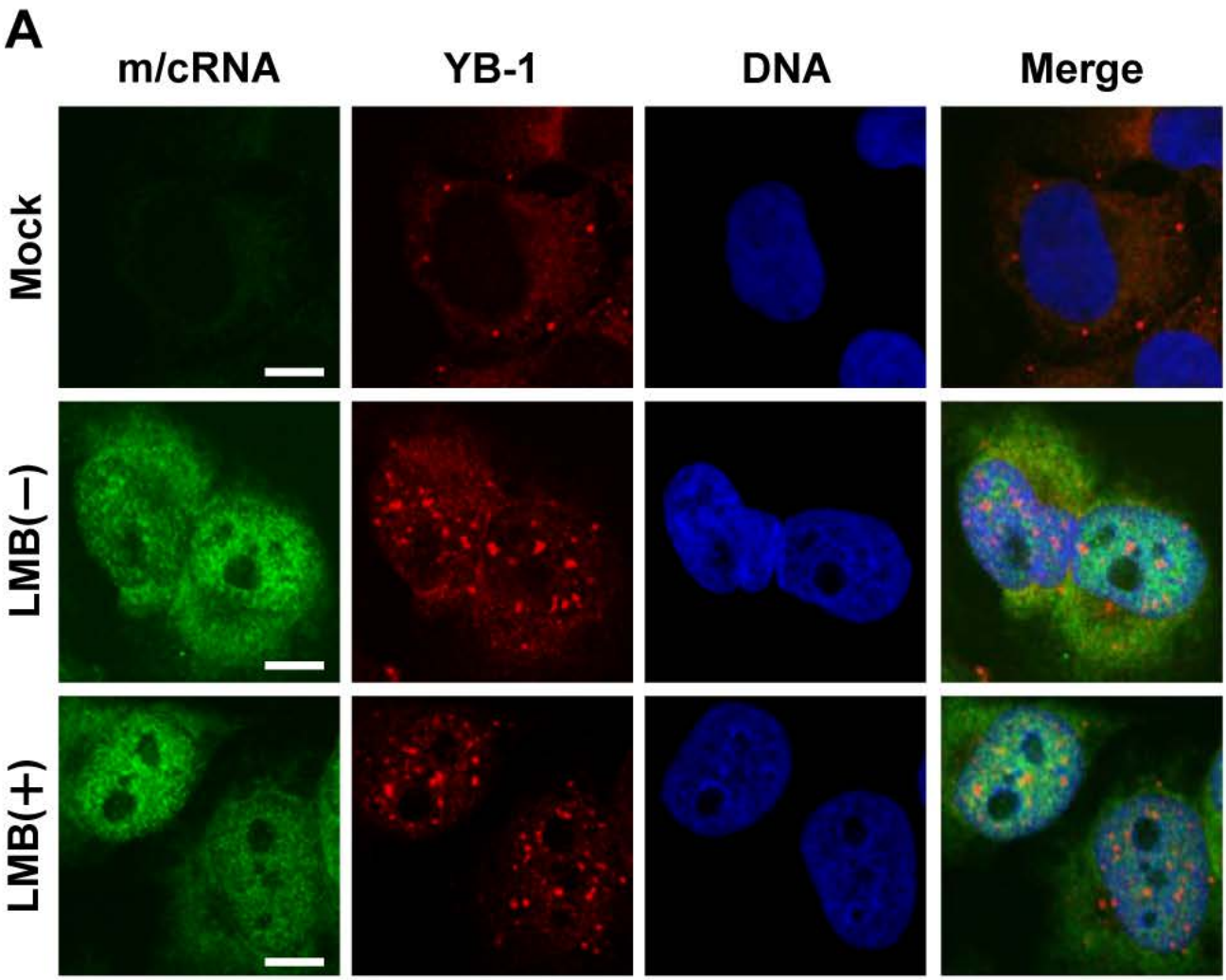

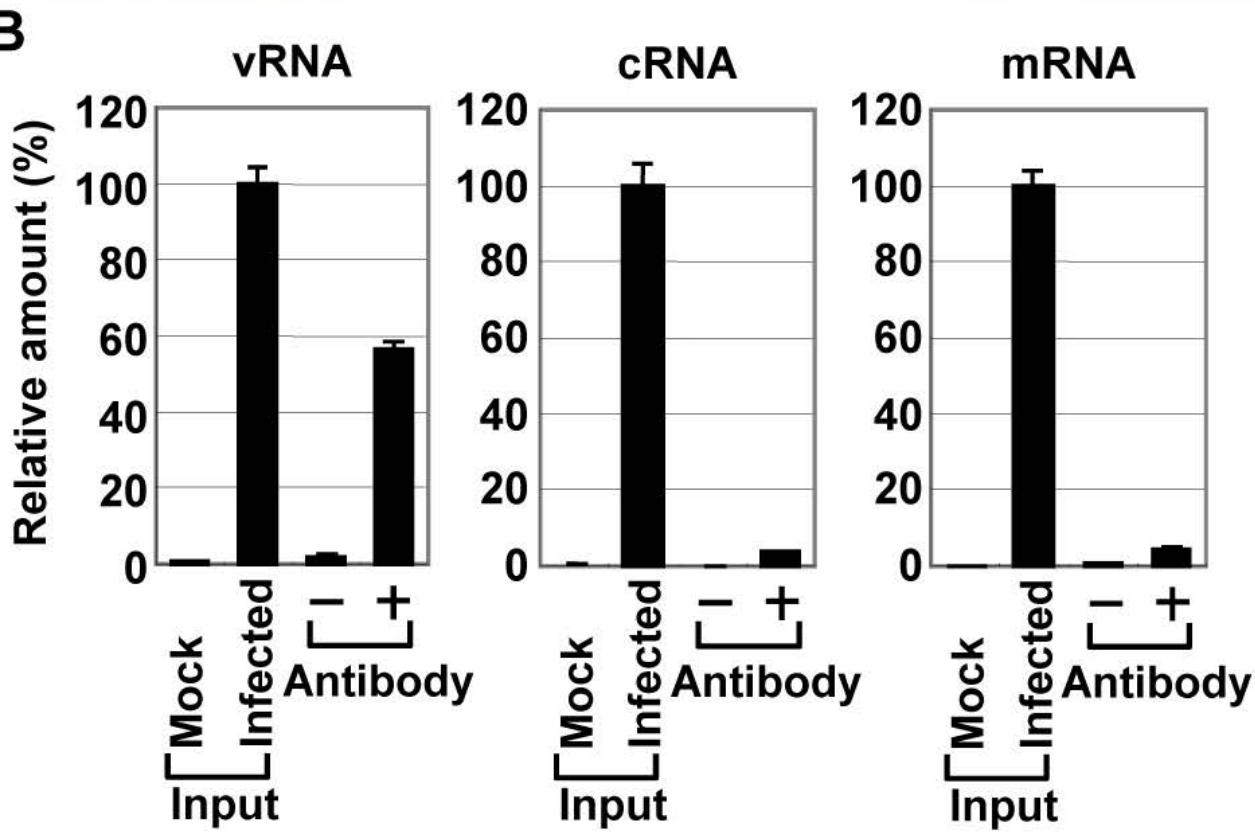

Kawaguchi et al., Figure 4

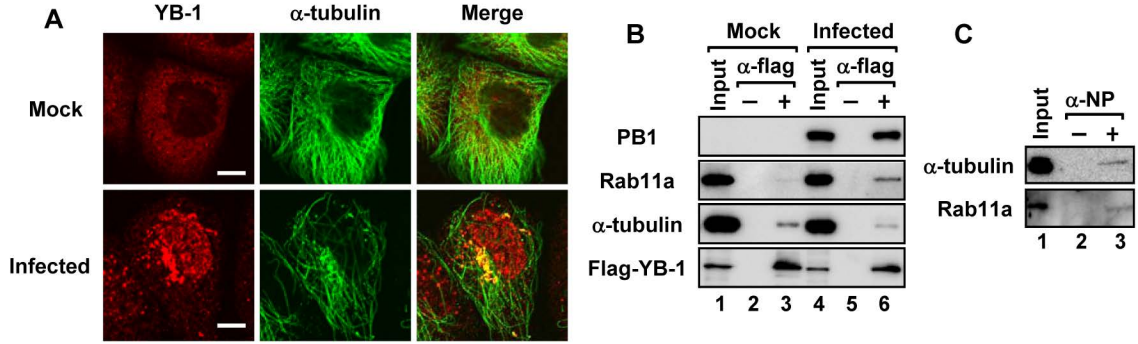

Kawaguchi et al., Figure 5

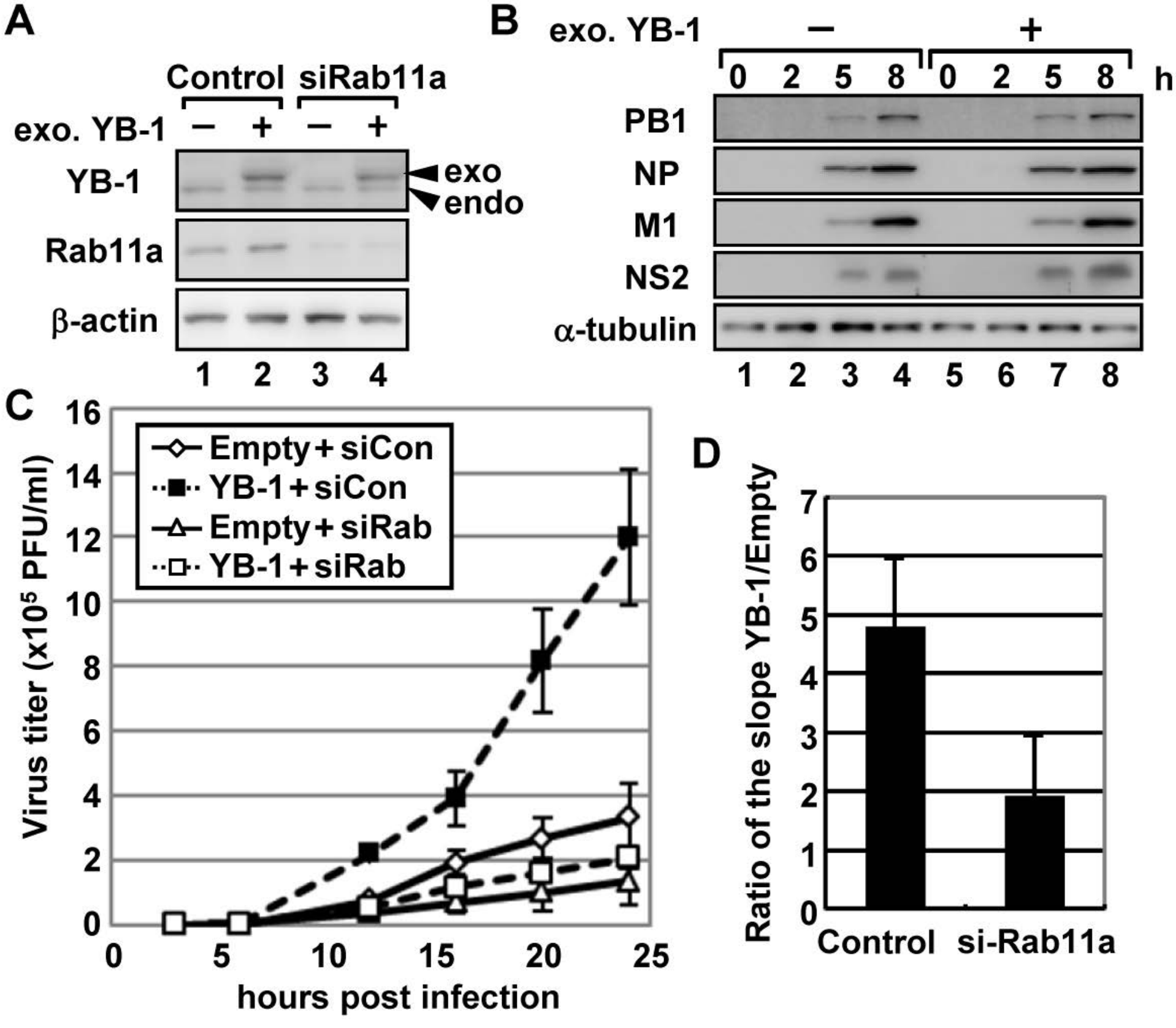

Kawaguchi et al., Figure 6

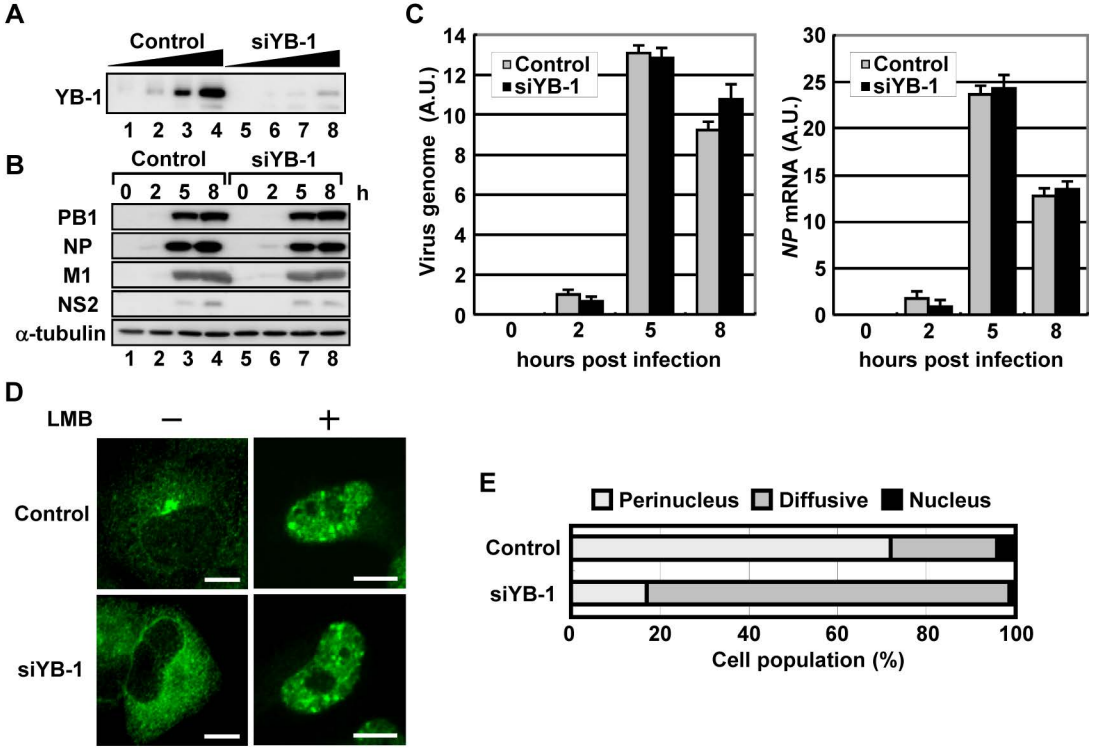

Kawaguchi et al., Figure 7